Proceedings of International Structural Engineering and Construction, 7(2), 2020
Emerging Technologies and Sustainability Principles
*Edited by* Askarinejad, H., Yazdani, S., and Singh, A.

ISSN: 2644-108X
www.doi.org/10.14455/ISEC.2020.7(2).STR-32

# FINITE ELEMENT ANALYSES ON CORRODED PONY TRUSS BRIDGE FOR REASONABLE MAINTENANCE

RISA FUJINAGA[1], TATSUMASA KAITA[1], RYOKO KOYAMA[2], TSUTOMU IMAI[3], and KATASHI FUJII[4]

[1]*Dept of Civil Engineering and Architecture, Tokuyama College of Technology, Shunan, Japan*
[2]*UBE Machinery Corporation, Ltd., Ube, Japan*
[3]*Road division, Dept of Construction, Shunan City Government Office, Shunan, Japan*
[4]*Graduate School of Engineering, Hiroshima University, Higashi-hiroshima, Japan*

The load bearing capacity of an existing corroded pony truss bridge, which is used for 100 years was estimated from FEM results for whole bridge model. The beam element model is to clarify that the influence of the residual out-of-plane deformation in main truss structures on the load bearing capacity from the viewpoint of whole bridge. Also, shell element model is to clarify that the influence of severe corrosion damages occurred in many structural members on the load bearing capacity as whole bridge. On the other hand, the influence of assumed support conditions in analytical models were discussed from the analytical results of both type of models, because it will be thought that the performance of shoes deteriorates gradually by long in-service period. The ultimate load bearing capacity was estimated by the critical live load magnification. From the analytical results, the residual out-of-plane deformation of main truss structures in this bridge had little influence on the ultimate load bearing capacity. Also, the ultimate load bearing capacity may decrease up to 20% due to aging deterioration of shoes including corrosion damages. In bridge maintenance, it should be paid attention on local severe corrosion damages on the structural member, which may occur higher secondary stress.

*Keywords*: Ultimate load bearing capacity, Support condition, Residual deformation, Local corrosion damage, Secondary stress, Live load magnification.

## 1 INTRODUCTION

Recently, the maintenance of aging steel bridges, which have serious corrosion damages becomes one of the important social problems in Japan. Especially, many local municipalities have strict conditions in terms of financial difficulties and human resources, and it is difficult to keep all the bridges in good condition. Therefore, it will be very important to estimate the remaining load-bearing capacity of the whole bridge as accurately as possible for drawing the safe and reasonable future planning.

If the remaining load-bearing capacity is estimated by finite element analysis, the numerical model must have a lot of analytical assumptions. In them, the support condition of the bridge has a tremendous influence load-bearing capacity of bridges. In these assumptions, though it will be thought that the support condition has an unignorable influence on the load-bearing capacity of the whole bridge, the actual pin and roller performance will be deteriorated by corrosion of pin, roller, and anchor bolts. Also, residual deformation by past earthquakes and flood disasters may exist in main structural members.

In this study, the load-bearing capacity of a corroded pony truss bridge used for about 100 years was estimated from FEM results for the whole bridge model. The beam element model is to clarify the influence of the residual out-of-plane deformation in main truss structures on the load-bearing capacity. Shell element model is to clarify that the influence of severe corrosion damages occurred in many structural members on the load-bearing capacity as the whole bridge. Moreover, the influence of assumed support conditions on ultimate load-bearing capacity was discussed from the analytical results of both type of models.

## 2 AGING PONY TRUSS BRIDGE FOR ANALYSIS

### 2.1 Outlines

The aging steel bridge to be analyzed is a Warren truss with curved chords and used for 100 years in the mountain area in the present location. All structural members are constructed by rivet joints combined with several simple-shaped steels and many racing bars. The main span is 29.3m and the clear width is 4.5m, as shown in Figure 1. It can be noticed that the maximum height of the main truss is kept as low as 2.9m from the considering of pony truss without lateral members.

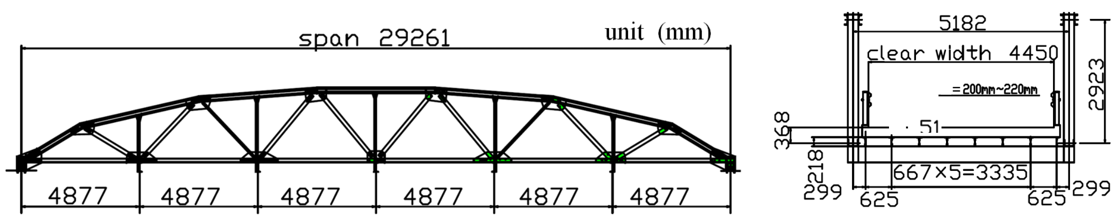


(a) Side view

(b) Sectional view

Figure 1. Dimensions of main span.

### 2.2 Field Investigation for Aging Deterioration

#### 2.2.1 *Corrosion damages*

In this bridge, it can be confirmed that various types of corrosion are distributed throughout the main truss members. On the upper flange of almost all upper chord members, many pitting corrosions, which are caused by painting deterioration, are found, as shown in Figure 2(a). Also, the joint part of upper chord members has groove-like corrosion at the boundary of the splice plate. These severe corrosion damages tend to be concentrated to center span because the upper chord member with no inclination has bad drainage performance of rainwater and dew condensation water. In the lower chord member near shoes Figure 2(b), it can be found large corrosion holes, which reach into about half of the initial cross-section area, because many clods of dirt, mosses, bait of carps are depositing on L-shape steels and connection plate.

All shoes are fixed directly to each pier using four anchor bolts through the baseplate as show in Figure 2(c). However, since severe defect of nut due to corrosion can be found in many anchor bolts, this damaged situation will indicate a high probability of occurring the uplift behavior and horizontal displacement. In that case, it is thought that the support condition in structural analysis should be assumed to actual condition, which will be like simply-support than fixed support.

(a) Pitting corrosions (b) Corrosion holes (c) Condition of shoes

Figure 2. Corrosion damages.

### 2.2.2 *Residual Out-of-plane deformation on main truss structures*

The main truss structures of this bridge have out-of-plane deformation, which occurred for a term of 100 years in-service period (Koyama *et al.* 2017). In this study, field measurement for out-of-plane deformation was carried out in 2016 and 2018 because it has possibilities to change the dimension of deformation by repair work, including member replacement in 2017.

Figure 3 shows the measurement results of out-of-plane deflection. It can be found that the main truss of the downstream side was deformed globally into S shape, and the upstream side deformed toward to the outside. Also, deformation amount in upstream side was decreased to about 1/2 than that of 2016. This fact may indicate that uncertain dead load stress was distributed into other structural members by partial member replacement under acting dead load. In the frame analyses in this study, out-of-plane deformation measured in 2018, are considered as the initial deformation of the main truss structure.

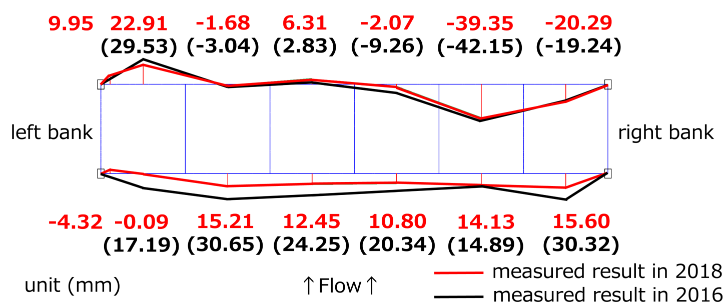


Figure 3. Measurement results of out-of-plane deformations on main truss structures.

## 3 3D FRAME ANALYSES USING BEAM ELEMENT

### 3.1 Whole Bridge Modeling and Analytical Conditions

In this study, the non-linear finite element analyses considering both geometrical and material nonlinearity studies were performed by using ABAQUS/Standard 6.14-5. In this whole bridge model with 5863 nodes, all main structural members are constructed by beam elements, and the panel points are rigid jointed. The length of each beam element was set to about 100mm. Based on the tensile tests, the material properties of the steel were assumed to be elastic modulus E=203.5 [GPa], yield stress $\sigma_y$=312.3 [MPa], and Poisson's ratio $\nu$=0.274. The stress-strain relation was set to the perfect elastoplasticity.

4 analytical cases were prepared depending on out-of-plane deformation and support conditions, as shown in Table 1. The dead load of RC-slab and live load were distributed as an external force on all stringers based on the influence lines for the reaction force of stringers. In

the case of this bridge, only primary load p2 in L live load based on Japan Specifications for Highway Bridges were considered to the analytical model because the heavy vehicles cannot pass to this bridge due to narrow corner clearance. Live load p2 was parametrically controlled by using the live load magnification α and was increased until α reaches the peak with some collapse of the analytical model. This live load magnification α means the safety factor of the whole bridge in the ultimate state.

### 3.2 Analytical Results and Discussions Focusing on Residual Out-of-plane Deformation

Table 2 shows the critical live load magnification $\alpha_{cr}$ (ultimate load bearing capacity) estimated from analytical results of 4 models in Table 1. The $\alpha_{cr}$ of Models-SS decreased by 14~20% than Models-FS with or without corrosion damages, because it will mean that the live load stress also increased on members other than upper chord members due to simply-support in Models-SS.

Figure 4 shows analytical results of Models-D1. From these figures, it can confirm that the Mises stress level on lower chord members of Model-D1-SS is higher than that of Model-D1-FS. However, though Model-D1-FS collapsed by local out-of-plane buckling of the upper chord member, both main truss structures leaned to inside when ultimate state in Model-D1-FS.

On the other hand, you can notice that the differences of $\alpha_{cr}$ between Models-D0 and D1 are no more than 4.4%. Therefore, it will be thought that the residual out-of-plane deformation of main truss structures shown in Figure 2 has little influence on the ultimate load bearing capacity as from the viewpoint of whole bridge.

Table 1. Analytical models using beam element.

| | Out-of-plane deformation | Support condition |
|---|---|---|
| Models | not considered(D0) | Fixed Support |
| | | Simple Support |
| | considered(D1) | Fixed Support |
| | | Simple Support |

Table 2. Critical live load magnification $\alpha_{cr}$.

| Models | D0 | D1 | Difference(%) |
|---|---|---|---|
| FS | 6.8 | 6.5 | 4.4 |
| SS | 5.5 | 5.6 | 1.8 |
| Difference(%) | 19.1 | 13.8 | |

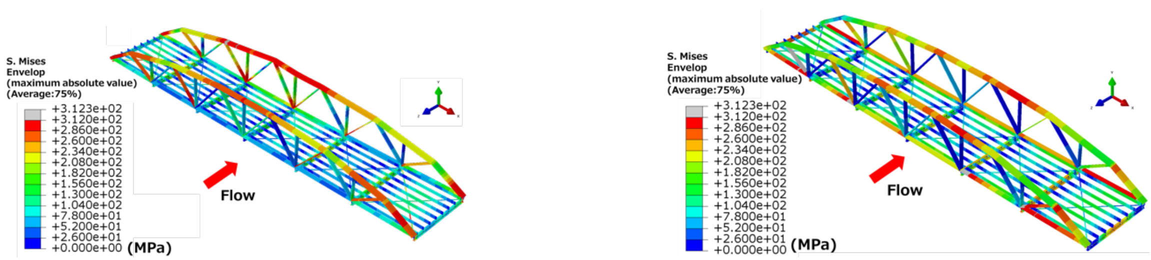


(a) Model-D1-FS ($\alpha_{cr}$=6.5) (b) Model-D1-SS ($\alpha_{cr}$=5.6)

Figure 4. Deformation (x 20) and Mises stress distribution in ultimate state.

## 4 INFLUENCE WITH LOAD BEARING CAPACITY OF CORROSION DAMAGES

### 4.1 Whole Bridge Modeling and Analytical Conditions

In this model, all main structural members are constructed by the shell element with 4 nodes, and all rivet joints were modeled as the rigid connection. The size of each shell element was set to under 40mm square to consider the corrosion damages, which have a certain area. In the corrosion modeling, the maximum corrosion depth was distributed to the entire corrosion area based on the results of field investigation. The stress-strain relation and the material properties of the steel are the same as the beam element model.

Four analytical cases were prepared depending on corrosion damages and support condition, as shown in Table 3. In these analytical models, the residual out-of-plane deformation was not included from the consideration of analytical results for the 3D frame model.

Table 3. Analytical models using shell element.

| | Corrosion damages | Support condition |
|---|---|---|
| Models | not considered(C0) | Fixed Support |
| | | Simple Support |
| | considered(C1) | Fixed Support |
| | | Simple Support |

## 4.2 Results and Discussions for Initial State Model (without Corrosion Damages)

Figure 5 shows the analytical results of Models-C0. From Figure 5(a), it can confirm that the plastic buckling of upper chord member at center span was appeared under the fixed support condition (Koyama et al. 2019). Moreover, the buckling point and $\alpha_{cr}$ were also close to them of Model-D1-FS shown in Figure 4(a).

However, Model-C0-SS reached the ultimate state by yielding at the boundary between the gusset plate and upper chord member on near each shoe, as shown in Figure 5(b). The reason for this will be thought that higher secondary stress was added by pin rotating as a simply-support condition.

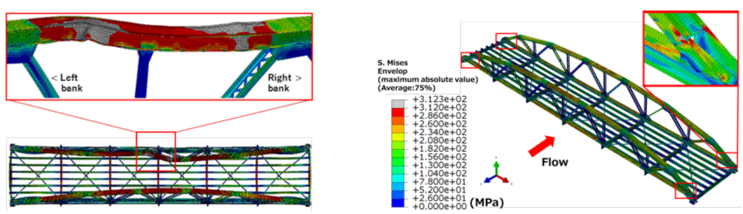


(a) Model-C0-FS ($\alpha_{cr}$=6.91) (x 20) (b) Model-C0-SS ($\alpha_{cr}$=4.7)

Figure 5. Deformation and Mises stress distribution in ultimate state.

## 4.3 Results and Discussions for Current State Model (with Corrosion Damages)

Figure 6(a) shows the ultimate state ($\alpha_{cr}$=4.2) of Models-C1-SS considering corrosion damages. In this model, the upper flange of upper chord members near the center span reached a yielding state locally due to thickness decreasing by severe pitting corrosions shown in Figure 2(a). It will be thought that the influence on secondary stress of thickness decreasing cannot be negligible because all yielding areas on upper flange were located very near the joint point between the upper chord member and counterbrace members. Furthermore, it can be found that the bending collapse of a lower chord member near the shoe occurs almost at the same time on the downstream side, as shown in Figure 6(b). Especially, yielding area in this chord member was identical with the location of corrosion holes shown in Figure 2(b).

Table 4 shows the critical live load magnification $\alpha_{cr}$ estimated from the analytical results of 4 models in Table 3. From the comparison of Model-C1-FS with Model-C1-SS, if it was assumed that the support condition was changed from fixed support to simply support due to aging deterioration, the ultimate load-bearing capacity, including the influence of current corrosion damages, may decrease up to 20%. On the other hand, for the rate of decrease in the ultimate load-bearing capacity by corrosion damages, it will be estimated that the case of assuming fixed support will be higher than simply-support.

In actually, though the intermediate behavior between fixed support and simply support will be appeared if the shoes become deteriorated with aging, there should be paid attention on the local severe corrosion damages on the structural member, which may occur higher secondary stress in bridge maintenance.

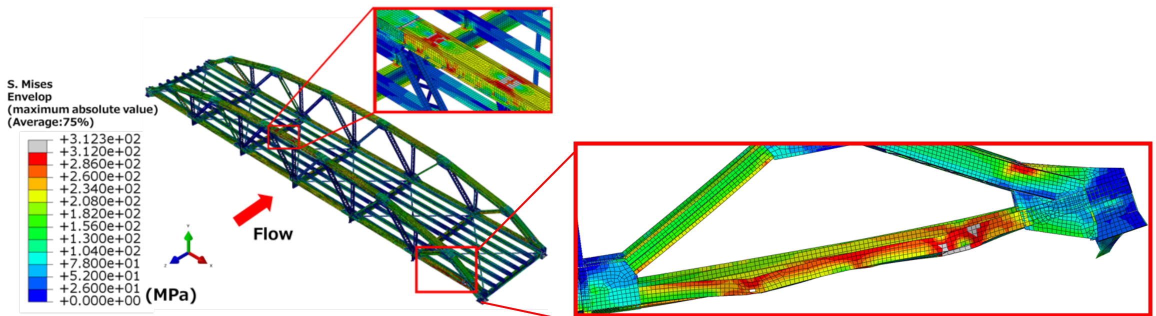


(a) Ultimate state ($\alpha_{cr}$=4.2) (b) End lower chord member

Figure 6. Deformation (x 20) and Mises stress distribution in ultimate state for Model-C1-SS.

Table 4. Critical live load magnification $\alpha_{cr}$.

| Models | C0 | C1 | Difference(%) |
|---|---|---|---|
| FS | 6.9 | 5.3 | 23.3 |
| SS | 4.7 | 4.2 | 10.6 |
| Difference(%) | 32.0 | 20.8 | |

## 5 CONCLUSIONS

1) The residual out-of-plane deformation of main truss structures in this bridge had little influence on the ultimate load-bearing capacity.
2) If it was assumed that the support condition was changed from fixed support to simply support due to aging deterioration, the ultimate load-bearing capacity, including the influence of current corrosion damages may decrease up to 20%.
3) In bridge maintenance, there needs to be paid attention on local severe corrosion damages, on the structural member, which may occur higher secondary stress.

## References

Koyama, R., Kaita, T., Yamane, T., Kaneshige, K., and Imai, T., *Analytical Estimation on Load Bearing Capacity for Aging Pony Truss Bridge Considering Actual Traffic Conditions*, Proceedings of the 15th East Asia-Pacific Conference on Structural Engineering and Construction (EASEC-15), 1914-1922, 2017.

Koyama, R., Kaita, T., Yamane, T., and Imai, T., *Analytical Estimation on Remaining Load Bearing Capacity of Aging Truss Bridge by Using Whole Bridge Modeling*, Proceedings of Bridge Engineering Institute Conference in 2019 (BEI-2019), Yail, J. K. (eds.), 714-718, 2019.